THE JOURNAL OF BIOLOGICAL CHEMISTRY VOL. 288, NO. 13, pp. 9058–9065, March 29, 2013
Published in the U.S.A.

Engineering Anthrax Toxin Variants That Exclusively Form Octamers and Their Application to Targeting Tumors*[S]

Received for publication, January 9, 2013, and in revised form, February 5, 2013 Published, JBC Papers in Press, February 7, 2013, DOI 10.1074/jbc.M113.452110

Damilola D. Phillips[‡], Rasem J. Fattah[‡], Devorah Crown[‡], Yi Zhang[‡], Shihui Liu[‡], Mahtab Moayeri[‡], Elizabeth R. Fischer[§], Bryan T. Hansen[§], Rodolfo Ghirlando[¶], Ekaterina M. Nestorovich[‖], Alexander N. Wein[‡], Lacy Simons[‡], Stephen H. Leppla[‡], and Clinton E. Leysath[‡1]

From the [‡]Laboratory of Parasitic Diseases, NIAID, National Institutes of Health, Bethesda, Maryland 20892, the [§]Electron Microscopy Unit, Research Technologies Branch, NIAID, National Institutes of Health, Hamilton, Montana 59840, the [¶]Laboratory of Molecular Biology, NIDDK, National Institutes of Health, Bethesda, Maryland 20892, and the [‖]Department of Biology, Catholic University of America, Washington, D. C. 20064

Background: Anthrax toxin protective antigen (PA) forms heptameric or octameric oligomers after proteolytic activation.
Results: We engineered two PA variants that form active octamers only when both versions are present.
Conclusion: These PA variants enlarged the therapeutic window when used to target tumors compared with previous systems.
Significance: This is the first method to generate a pure pool of octameric PA oligomer.

Anthrax toxin protective antigen (PA) delivers its effector proteins into the host cell cytosol through formation of an oligomeric pore, which can assume heptameric or octameric states. By screening a highly directed library of PA mutants, we identified variants that complement each other to exclusively form octamers. These PA variants were individually nontoxic and demonstrated toxicity only when combined with their complementary partner. We then engineered requirements for activation by matrix metalloproteases and urokinase plasminogen activator into two of these variants. The resulting therapeutic toxin specifically targeted cells expressing both tumor associated proteases and completely stopped tumor growth in mice when used at a dose far below that which caused toxicity. This scheme for obtaining intercomplementing subunits can be employed with other oligomeric proteins and potentially has wide application.

Bacillus anthracis is a Gram-positive, spore-forming bacterium that is the causative agent of anthrax. Anthrax disease is mediated by the tripartite toxin (2, 3) and the poly-D-glutamic acid capsule of the bacterium (1). The toxin is composed of protective antigen (PA),[2] lethal factor (LF), and edema factor. PA binds to the cellular receptors CMG2 and TEM8, and the 83-kDa PA protein is cleaved by furin to a 63-kDa form (PA_{63}), which then oligomerizes. Formation of an oligomer generates LF/edema factor binding sites at the interface of two adjacent PA molecules. PA oligomerization also initiates receptor-based signaling that triggers endocytosis of the complex. Upon acidification of the endosome, the PA oligomer forms a pore in the endosomal membrane through which the LF and edema factor proteins transit. Once in the cytosol, these effector proteins exert their catalytic activities. Edema factor is a calmodulin-dependent adenylyl cyclase (4) that aids in dissemination of *B. anthracis* in the host (5). LF is a zinc metalloprotease that cleaves mitogen-activated protein kinase kinases (6, 7) and NLRP1 (8), thereby perturbing signal transduction in host cells.

It has long been observed that PA forms a heptamer upon furin cleavage and that oligomerization is required for toxicity (9). Recently, Krantz and colleagues (10) showed that PA is also able to form functional octamers. Conditions under which octameric oligomerization predominates were exploited to crystallize the octamer (10). Comparison of the octamer and heptamer crystal structures revealed that there are two orientations of PA domain 4 (the receptor-binding domain) that alternate in the octamer to accommodate the new geometry. Constraining the location of PA domain 4 using different linkers connected to the remainder of the protein altered the proportion of octamers and heptamers (11).

We set out to create PA variants that would selectively and exclusively form octamers, starting with the PA mutant D512K (12), which is incapable of forming oligomers (see Fig. 1*A*). We prepared a library of PA variants having the D512K substitution together with random mutations in several residues on the complementary face of PA_{63} within the oligomers (see Fig. 1*B*) and screened for a (re)gain of function. Screening of this library successfully identified mutations that complement D512K. We next placed D512K and the new complementary mutations into two separate PA proteins, so that formation of oligomers through the use of the two unique interfaces (wild type and mutated) resulted in only even-numbered oligomers, among which octamer was expected to predominate (Fig. 1*C*). Furthermore, we applied the octamer strategy to create a tumor-targeting agent that had high specificity and efficacy.

EXPERIMENTAL PROCEDURES

Plasmids—Plasmid pYS2-PA-D512K was created through site-directed mutagenesis of pYS2 (13) by GM Biosciences

* This work was supported in part by the Intramural Research Programs of NIAID and NIDDK from the National Institutes of Health.
[S] This article contains supplemental "Experimental Procedures," "Results," Tables S1 and S2, Figs. S1–S4, and additional references.
[1] To whom correspondence should be addressed: Microbial Pathogenesis Sect., Laboratory of Parasitic Diseases, National Institute of Allergy and Infectious Diseases, National Institutes of Health, 9000 Rockville Pike, Bethesda, MD 20892. Tel.: 301-402-0730; Fax: 301-480-3633; E-mail: leysathce@niaid.nih.gov.
[2] The abbreviations used are: PA, protective antigen; LF, lethal factor.

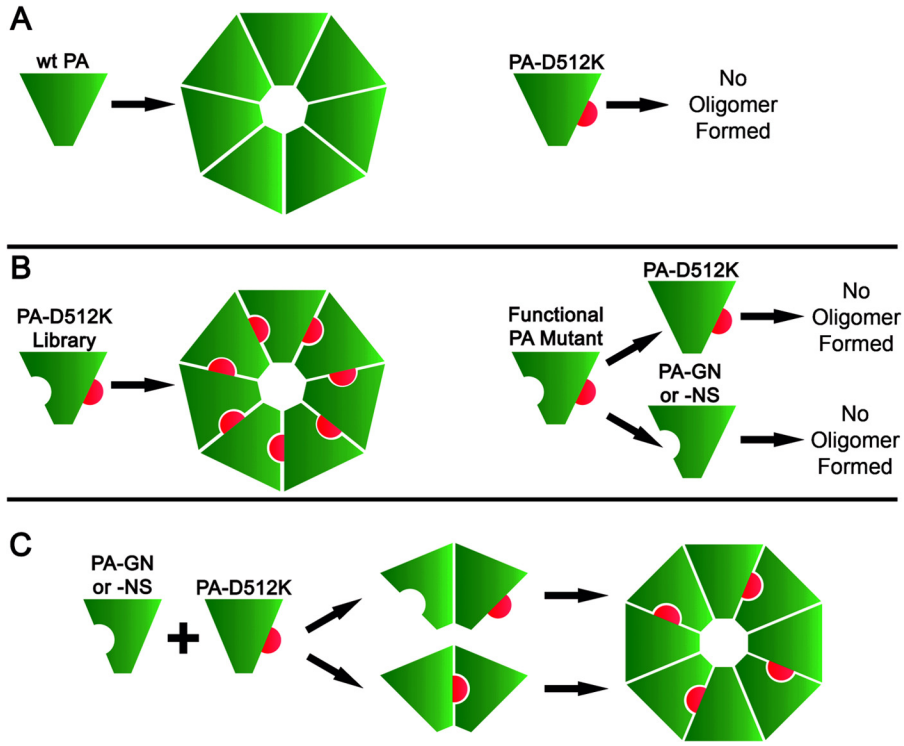

FIGURE 1. **Scheme for discovery of PA mutants that exclusively form octamers.** *A*, wild type PA oligomerizes to predominantly form heptamers, whereas point mutant PA-D512K is oligomerization-deficient. *B*, a library was created using PA-D512K by introducing diversity at residues on the complementary binding surface to the face of PA that contains the D512K mutation and screened for variants that possessed gain of function mutations. After successful isolation of the functional PA variants, separation of the mutations from D512K was necessary to confirm that the substitutions were individually loss of function mutations. *C*, combining both complementary PA variants allows formation of oligomers using two unique interfaces (wild type and engineered). This allows the formation of only even-numbered oligomers, in which octamers predominate.

(Rockville, MD). The *pagA* gene fragment containing the D512K point mutation between the PstI and BamHI sites was moved into pYS5 (13) by digestion of both vectors with PstI and BamHI with additional cleavage of the pYS5 *pagA* gene with SwaI and cleavage of the pYS2-PA-D512K vector backbone with FspI (blunt cutting enzymes were used to prevent alternative ligation products) followed by ligation. Plasmids were electroporated into *Escherichia coli* XL1-Blue (Agilent Technologies, Santa Clara, CA), sequenced, then electroporated successively into *E. coli* strain SCS110 (Agilent Technologies) and BH460, an acapsular, nontoxogenic, protease-deficient, protein overexpression *B. anthracis* strain (14).

Reversion of the D512K point mutation to wild type in PA variants recovered from the screen was performed with QuikChange multisite-directed mutagenesis kit (Agilent Technologies) using the manufacturer's instructions. The primer used for reversion was GGATAGCGGCGGTTAATCCTAGTGATCCATTAGAAACGACTAA. Vectors used to express PA-L1-GN, PA-L1-NS, and PA-U2-D512K were constructed by placing D512K or the newly isolated mutations into existing PA variants PA-L1 and PA-U2 using QuikChange multisite-directed mutagenesis kit in a similar manner. PA-U2-D512K was constructed using GGATAGCGGCGGTTAATCCTAGTAAGCCATTAGAAACGACTAA with pYS5-PA-U2. PA-L1-GN and PA-L1-NS were constructed using pYS5-PA-L1 with GGTTACAGGACGGATTGATGGAAATGTATCACCAGAGGCAAACCACCCCCTTG and GGTTACAGGACGGATTGATAACAATGTATCACCAGAGGCAAGCCACCCCCTTG, respectively.

Proteins—PA variants (15), LF (16), and FP59 (15) were expressed and purified as described previously. Expected molecular weights of all proteins were confirmed by electrospray ionization mass spectrometry. FP59 is a fusion protein of the N-terminal 254 amino acids of LF, which is the PA-binding domain, fused to the catalytic domain of *Pseudomonas* exotoxin A, which ADP-ribosylates eukaryotic elongation factor 2 to inhibit protein synthesis, leading to cell death. This fusion protein has been shown to be more toxic to most cells than LF in combination with PA. Toxin doses used in these studies were selected based on previous work.

Library Construction, Screening, and Tissue Culture Studies—The library containing RRM degenerate codons at PA amino acid positions Lys-238, Arg-242, Lys-245, and Arg-252 was constructed using overlap extension PCR (17). Inner primers were CTTCTGATCCGTACAGTGATTTCGAARRMGTTACAGGARRMATTGATRRMAATGTATCACCAGAGGCARRMCACCCCCTTGTGGCAGC (forward) and TTCGAAATCACTGTACGGATCAGAAG (reverse), whereas outer primers used for both primary and secondary amplifications were GACGAGCGCTTCGGTCTTAACTG (forward) and AGCAGCCAACTCAGCTTCCTTTCG (reverse). The amplicon was cut with BstXI and BamHI and ligated into pYS5-PA-D512K. Purified plasmid was transformed successively into electrocompetent cell strains MC1061 (ATCC, Manassas, VA), SCS110, and BH460. At each step, transformed cells were placed at 37 °C overnight on LB agar plates containing 100 μg/ml carbenicillin for *E. coli* strains, and 10 μg/ml kanamycin for BH460. After overnight growth, plates were scraped, and

plasmid was isolated. Transformation into MC1061 produced a library of 4×10^5 clones, a 97-fold coverage of the theoretical library size. Introduction into SCS110 gave 2.5×10^4 clones or 6-fold coverage. Each single electroporation reaction into BH460 yielded 400 colonies, or ~0.1-fold library coverage. BH460 colonies were picked and placed into individual wells of 96-well plates (Corning) and grown overnight at 37 °C in FA medium (13). Plates were centrifuged to pellet the bacteria, and 2 μl was withdrawn from each well for screening.

RAW264.7 cells, a mouse macrophage cell line, were used to assess toxicity of PA variants. Cells were plated the night before a screening experiment at 50,000 cells per well and grown overnight at 37 °C in a humidified atmosphere with 5% CO_2 in Dulbecco's modified Eagle's medium (DMEM) with Glutamax (Invitrogen) supplemented with 10% fetal bovine serum, 10 mM HEPES buffer, pH 7.3, 1 mM sodium pyruvate, and 10 μg/ml gentamycin (complete DMEM). The following day, the supernatant was aspirated, and 100 μl of complete DMEM supplemented with 1.8 nM FP59 was placed on the cells in addition to the 2 μl of BH460 supernatant per well. Plates were placed at 37 °C for 24 h, and then viability was assessed using a 1-h incubation at 37 °C with the addition of 25 μl of complete DMEM supplemented with 2.5 mg/ml 3-(4,5-dimethyl-2-thiazolyl)-2,5-diphenyl-2*H*-tetrazolium bromide. After aspiration of the supernatant, thiazolium salts were solubilized in 91% isopropanol, 0.038 M HCl, and 0.476% SDS and then read at 570 nm. Tissue culture studies were performed similarly but with purified PA variants mixed with FP59 instead of bacterial supernatants and in the presence or absence of protease inhibitors. Nafamostat mesylate (Sigma) was used at a concentration of 75 μM, whereas ilomastat (U. S. Biological, Swampscott, MA) was used at a final concentration of 25 μM.

Animal Studies—Balb/cJ and C57BL/6J mice (8–12 weeks old, female, 20–25 g) were purchased from The Jackson Laboratory (Bar Harbor, ME). For survival studies with LF as effector, Balb/cJ mice ($n = 10$/group) were injected intravenously (i.v., 200 μl) with single PA variants (50 μg) + LF (50 μg). When the two PA variants were tested in combination, each variant was used at 25 μg (for a total of 50 μg of PA) and combined with LF (50 μg). For survival studies with FP59 as effector, C57BL/6J mice were injected intraperitoneally (i.p., 1 ml) with single PA variants (10 μg) + FP59 (10 μg). When two PA variants were tested in combination, each variant was used at 5 μg (for a total of 10 μg of PA) and combined with FP59 (10 μg). In experiments to test toxicity of the PA variants in the absence of effector proteins, the same dose of PA described above were injected into mice without LF or FP59. Animals were observed every 8–12 h for signs of malaise over a 7-day period.

For tumor studies, female, age-matched nude mice (NCI-Frederick Mouse Repository) were injected intradermally with 1×10^6 or 5×10^6 A549 cells, and tumor growth was monitored. When tumors reached ~ 50 mg, mice ($n = 10$) were injected i.p. with six doses of either PBS or PA variants and LF in a 2:1 mass ratio of PA:LF on days 0, 2, 4, 7, 9, and 11. Tumor size and body weight were measured on these days. When testing a combination of two PA variants, a 1:1:1 mass ratio of PA variant 1:PA variant 2:LF was administered. One animal died under anesthesia and was removed from the study. Maximum tolerated dose studies were conducted using an identical administration schedule with C57BL/6J and nude mice, and blood chemistry analysis was conducted by the Clinical Center (NIH). All mouse experiments were performed under protocols approved by the Animal Care and Use Committee of the National Institute of Allergy and Infectious Diseases (National Institutes of Health).

Electron Microscopy and Image Analysis—Aliquots of PA oligomer preparations (5 μl) were briefly applied to freshly glow-discharged, carbon-coated, 200 mesh copper grids, and excess was removed by wicking with filter paper. Grids were then stained for 2 min with Nano-van (Nanoprobes, Inc., Yaphank, NY) and prepared and examined under cryo conditions at 300 kV with a FEG Titan Krios transmission electron microscope (FEI, Hillsboro, OR). Images were recorded at a nominal magnification of 120,000X and an electron dose of ~300 $e^-/Å^2$ to prevent radiation damage. Particles having axial orientation with a defocus range of ~0.5–2.5 μm were boxed with EMAN2 and then processed using the standard multireference free alignment to produce class averages with full contrast transfer function correction without imposed symmetry.

Analytical Ultracentrifugation—Samples of PA and its complex with LF were prepared in 0.3 M NaCl, 0.01 M Bis-Tris propane (pH 9.0) and 0.5 mM EDTA. Sedimentation velocity experiments were conducted at 20.0 °C on a Beckman Coulter ProteomeLab XL-I analytical ultracentrifuge. Samples of 400 μl were loaded in two-channel centerpiece cells and analyzed at a rotor speed of 25,000 rpm with data collected using both the absorbance and Rayleigh interference optical detection systems. In the latter case, data were collected as single scans at 250 nm using a radial spacing of 0.003 cm. Absorbance and interference data were individually analyzed in SEDFIT (version 12.7; Ref. 18) in terms of a continuous $c(s)$ distribution of Lamm equation solutions using an uncorrected s range of 0.0–30.0 S with a resolution of 300 and a confidence level of 0.68. In all cases, excellent fits were obtained with absorbance and interference r.m.s.d. values of 0.0026–0.0090 (A_{280}) and 0.0054–0.015 (fringes), respectively. Absorbance and interference data for wild type PA alone and combined with LF were also analyzed globally in SEDPHAT (version 9.4) (19) in terms of a hybrid continuous $c(s)$ distribution and global discrete species representing the major component. Solution densities ρ were measured at 20.000 °C using an Anton Paar DMA 5000 density meter, solution viscosities η were measured at 20.00 °C on an Anton Paar AMVn rolling ball viscometer, and protein partial specific volumes ν were calculated in SEDNTERP (version 1.09) (20) based on the amino acid sequence.

RESULTS

A library was constructed by partially randomizing several codons in a plasmid encoding PA-D512K. Amino acid substitutions at the positions selected could potentially complement the D512K mutation on an adjacent monomer within the oligomer, restoring the ability to form functional oligomers. Such "gain of function" mutations are easier to identify within a library in which all other members are inactive. As it was feasible to survey only a few thousand clones for toxicity, we designed a library that would contain <5,000 members. We

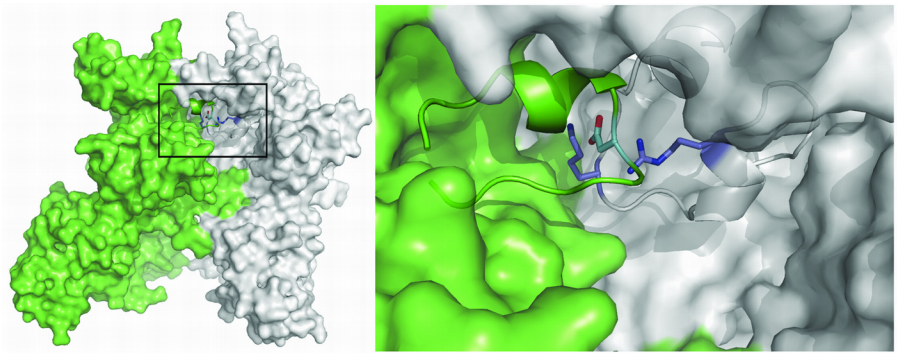

FIGURE 2. **Locations of mutated residues at the interface of two PA_{63} molecules.** An illustration of two adjacent PA_{63} monomers (one in *green*, the other in *white*) was made using the crystal structure of the PA pre-pore (Protein Data Bank code 1TZO) (31). Each PA molecule is rendered as a surface, whereas the *green loop* containing residue Asp-512 as well as the *white loop* containing residues Lys-245 and Arg-252 are rendered in schematic form for the sake of clarity. Asp-512 is colored *light blue*, whereas residues Lys-245 and Arg-252 are colored *dark blue*.

anticipated that charge reversal mutations were most likely to achieve complementation of the PA-D512K mutation. Examination of the crystal structure of the heptameric oligomer identified four positively charged residues on the opposite face of PA within 6 Å of the D512K mutation as candidate residues for mutation. We focused on the portion of the codon table that would lead to charge reversal (supplemental Fig. S1). By using a degenerate RRM codon (with R = A or G, and M = A or C), seven amino acid residues were accessed using eight different codons: aspartic acid, glutamic acid, lysine, arginine, asparagine, serine, and glycine. This focused library contained a total of 4,096 codons at the DNA level ($8^4 = 4{,}096$), coding for 2,401 unique proteins ($7^4 = 2{,}401$).

Individual colonies from the library were grown in 96-well plates, and supernatants containing the ectopically expressed PA variants were mixed with FP59 and placed on RAW264.7 cells to assess toxin function. (FP59 is a fusion protein of the N-terminal PA binding domain of LF with the catalytic domain of *Pseudomonas* exotoxin A.) After screening 1,500 transformants, two gain of function mutants were identified. Each contained substitutions at residues 245 and 252. The locations of these residues relative to residue 512 are shown in Fig. 2. The proteins were purified and characterized in assays containing FP59 (Fig. 3*A*). In toxicity assays, wild type PA gave an EC_{50} of 2.9 pM, whereas PA K245G/R252N/D512K (abbreviated as PA-GNK, EC_{50} = 5.6 pM) was 1.9-fold less toxic than wild type PA, and PA K245N/R252S/D512K (abbreviated as PA-NSK, EC_{50} = 10.3 pM) was 3.5-fold less toxic than wild type PA.

Complementary PA variants were next constructed by removing the D512K point mutation from the coding sequence of the doubly mutated proteins. PA-D512K and the two PA variants, referred to as PA-GN and PA-NS, were found to be non-toxic at concentrations 1,000-fold greater than the EC_{50} of wild type PA (Fig. 3*B*). However, combining PA-D512K with either PA-GN or PA-NS generated high toxicity comparable to that of wild type PA, yielding EC_{50} values of 3.9 pM, 9.4 pM, and 12.2 pM for wild type PA, PA-D512K + PA-GN, and PA-D512K + PA-NS, respectively (Fig. 3*C*). The putative octameric species were not toxic without an effector protein (Fig. 3*D*). Similar results were obtained by *in vivo* toxicity studies in mice, where only mixtures of two complementary variants were toxic when administered with either FP59 or LF (Fig. 3, *E* and *F*).

Biophysical characterization confirmed that octameric species were formed upon mixing the two complementary PA variants. Preformed heptamer combined with LF and the octamer complex formed in the presence of LF migrated differently by native gel electrophoresis (Fig. 4). Dynamic light scattering measurements of oligomers composed of wild type PA, PA-D512K + PA-GN + LF, and PA-D512K + PA-NS + LF revealed that each sample was monodisperse, so that only one oligomeric species was present per sample (supplemental Fig. S2). Sedimentation velocity experiments yielded a sedimentation coefficient distribution ($c(s)$) profile for wild type PA oligomer indicative of a major species at 14.58 ± 0.01 S (Fig. 5*A*), corresponding to an estimated molar mass of 520 ± 10 kDa, which is somewhat larger than the expected mass of the PA heptamer (M_{calc} = 444 kDa). Similarly, sedimentation data for the wild type PA + LF complex indicated the presence of a major species at 17.18 ± 0.08 S, along with what appears to be free PA heptamer. The estimated molar mass of 700 ± 20 kDa is consistent with the expected stoichiometry of seven PA_{63} units carrying 3 LF molecules (M_{calc} = 715 kDa). The PA-D512K + PA-GN + LF species gave a sedimentation coefficient of 21.22 ± 0.05 S and an estimated molar mass of 950 ± 30 kDa, whereas the PA-D512K + PA-NS + LF preparation has a sedimentation coefficient of 21.50 ± 0.03 S and an estimated mass of 905 ± 35 kDa, both close to the expected 868-kDa mass of eight PA_{63} moieties with four LF molecules.

Evidence of octameric assembly was obtained by use of electron microscopy (EM) (Fig. 5*B*) and by electrophysiological measurements (supplemental Fig. S3). Specimens negatively stained and imaged by cryo-EM clearly demonstrated heptameric and octameric species in the wild type and complementary variant samples, respectively. Analysis of at least 131 independent, obviously intact and axially oriented oligomers from each sample by reference free alignment revealed that both complementary variants assembled only as octameric species, whereas wild type PA generated heptameric species (Fig. 5*B*). Analyses in artificial lipid bilayers confirmed that the complementary pairs of PA variants formed ion-conducting channels that were similar to, but distinguishable from, those produced by wild type PA (supplemental Fig. S3).

The requirement that two PA variants combine to produce toxicity offered a strategy to create tumor-targeting agents of

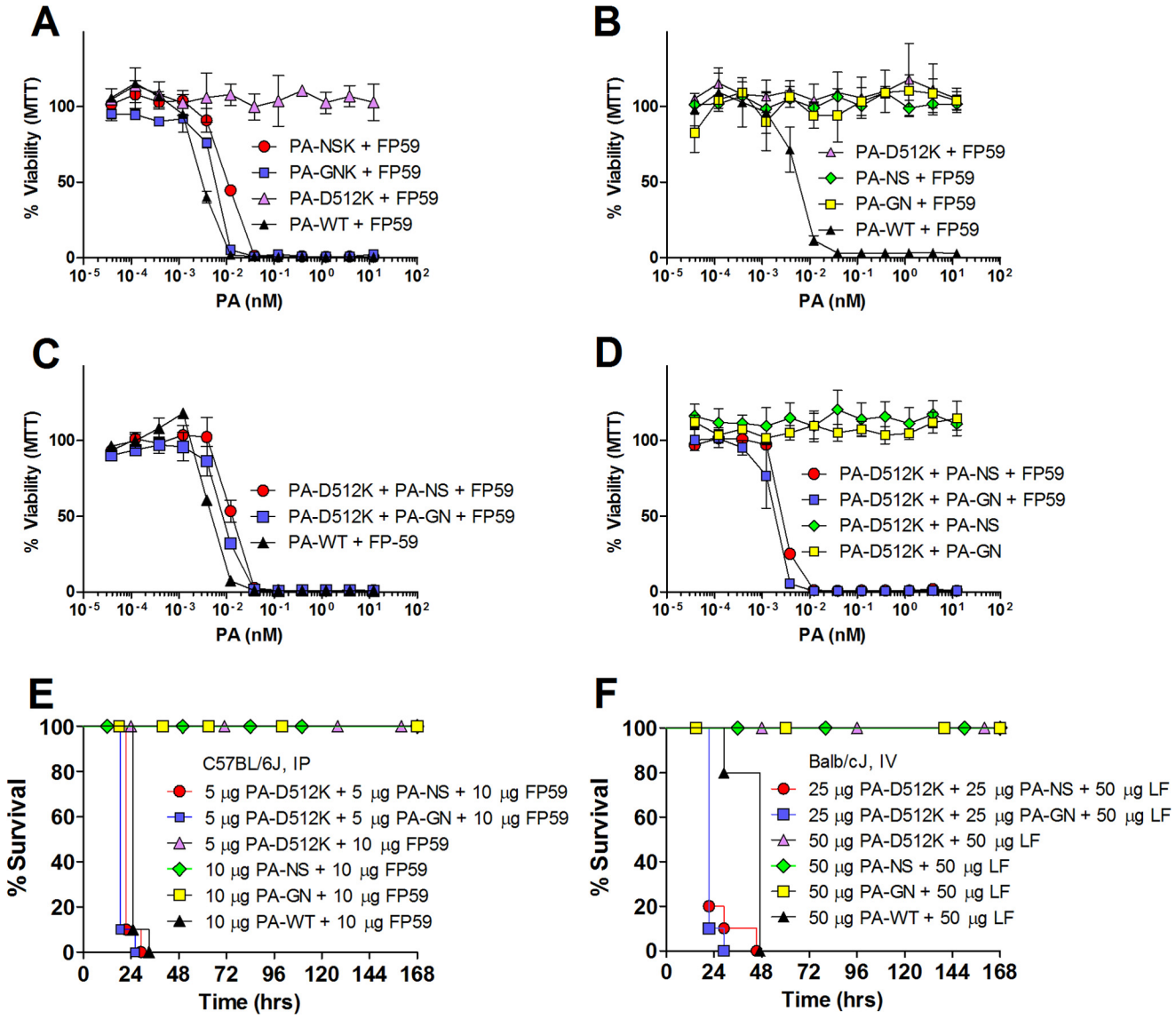

FIGURE 3. ***In vitro* and *in vivo* toxicity studies of PA variants.** *In vitro* toxicity studies were performed by exposing 50,000 RAW264.7 cells/well to varying concentrations of PA with 1.8 nM FP59 (a fusion protein composed of the N-terminal PA-binding domain of LF linked to the catalytic domain of *Pseudomonas* exotoxin A) for 24 h. Viability was then measured by 3-(4,5-dimethyl-2-thiazolyl)-2,5-diphenyl-2*H*-tetrazolium bromide (*MTT*) assay. Experiments were performed in triplicate, and *error bars* denote S.D. Concentrations are for the total PA concentration if two variants are mixed. *A*, toxicities were assessed for PA variants isolated from the library. *B*, toxicities of complementary PA variants were determined. *C*, combinations of complementary PA variants were compared with wild type PA. *D*, complementary PA variants were administered in the presence or absence of FP59. *E* and *F*, for *in vivo* tests, PA variants were administered intraperitoneally or intravenously either individually or in combinations to C57BL/6J (*E*) or Balb/cJ (*F*) mice ($n = 10$/group) together with FP59 or LF, and animal survival was monitored. Mouse survival times following all PA wild type and combination treatments were significantly different from single variant controls ($p < 0.0001$) using a log rank test.

increased specificity. In a previous work, we created PA variants in which the furin activation sequence was replaced by sequences cleaved by either urokinase plasminogen activator (*i.e.* PA-U2) (21) or matrix metalloproteases (*i.e.* PA-L1) (22), two proteases that are overexpressed by numerous tumors. These variants contained additional mutations so that PA-U2 and PA-L1 monomers had to be adjacent within an oligomer to form native LF binding sites (23). However, significant toxicity was still observed for each individual protein, as these mutations did not completely eliminate LF binding in the homo-oligomers. In contrast, introducing the D512K and GN or NS mutations into PA-U2 (PA-U2-D512K) and PA-L1 (PA-L1-GN or PA-L1-NS), respectively, produced a targeting system having an absolute requirement for both proteases to intoxicate a target cell. This result was observed, with a pair of complementary proteins (7.5 μg of PA-L1-GN + 7.5 μg of PA-U2-D512K + 7.5 μg of LF) completely inhibiting tumor growth, whereas the individual proteins had no effect, allowing tumors to grow at the same rate as those treated with PBS (Fig. 6*A*). No toxicity was observed, and there were no decreases in body weight in any experimental condition (Fig. 6*A*). Comparison of the previous intercomplementing format with the new octameric delivery system in the nude mouse tumor model using A549 cells with a dose of 50 μg of total PA variants with 25 μg of LF showed that both systems were equally effective at decreasing tumor size, whereas much less toxicity was induced by the octameric system (Fig. 6*B*).

Tissue culture experiments showed that toxicity was effectively eliminated when either protease activity was blocked, as was achieved using ilomastat (a matrix metalloprotease inhibitor) or nafamostat mesylate (an inhibitor of serine proteases of the class encompassing urokinase plasminogen activator) (supplemental Fig. S4). It was also found that C57BL/6J mice were able to tolerate six doses of 80 μg of complementary PA variants (40 μg of PA-L1-GN + 40 μg of PA-U2-D512K) with 40 μg of LF (supplemental Table S1), whereas the same dose of the previously described PA-U2 + PA-L1 intercomplementing proteins caused three of five animals to succumb, thereby establishing an approximate LD_{50} for the intercomplementing system. A doubling of the dose to 80 μg of PA-U2-D512K + 80 μg of PA-L1-GN + 80 μg of LF resulted in four of seven mice surviving, thereby identifying an approximate LD_{50} for the octameric system. All control animals that received 80 μg of wild type PA with 40 μg of LF succumbed after two doses. Serum from eight surviving animals in the maximum-tolerated dose study revealed that all samples contained normal levels of blood urea nitrogen and creatinine (supplemental Table S2). Alanine aminotransferase levels were all <60 units/liter (normal range is 17–77 units/liter), and all but one animal had aspartate aminotransferase levels below 120 units/liter (normal range, 54–298 units/liter). This animal received the highest dose of toxin (160 μg of PA-U2-D512K + 160 μg of PA-L1-GN + 160 μg of LF) and exhibited an aspartate aminotransferase level of 317 units/liter, which is elevated but still not at a level indicating liver damage.

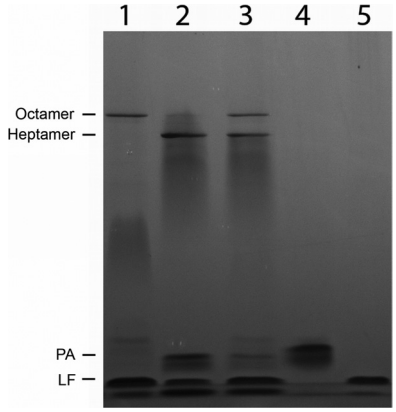

FIGURE 4. **Native gel electrophoresis of PA oligomers.** Electrophoresis of protein complexes were performed as described under "Experimental Procedures" (32). Samples are cleaved PA-GN + cleaved PA-D512K + LF (*lane 1*), cleaved wild type PA + LF (*lane 2*), samples 1 and 2 mixed immediately before electrophoresis (*lane 3*), uncleaved wild type PA (*lane 4*), and LF (*lane 5*).

DISCUSSION

In this work, we successfully engineered PA so that two complementary variants of PA were required to produce a functional octamer. We characterized these octamers by several biophysical techniques and showed that they possess near-wild type toxicity *in vitro* and *in vivo* when combined but are nontoxic individually. Additionally, we applied this system to require that two proteases act separately to activate a functional toxin complex. The protease-activated protein mixture completely halted tumor growth in a mouse model, whereas individual components had no observable toxicity. When compared with the previous intercomplementing system (23), the octameric system was found to have equal efficacy with significantly lower toxicity.

As mentioned earlier, our expectation was that negatively charged amino acids would be selected to complement the charge reversal at position D512K. Instead, the screen produced complementary mutations where positively-charged residues were replaced by small uncharged amino acids, *e.g.* K245G, K245N, R252N, and R252S. This result showed that shape complementarity to accommodate the lysine mutation (D512K) was the most important factor, as all selected amino acids (Gly, Asn, and Ser) were considerably smaller than the lysines or arginines that they replaced. The library created and screened in this work was relatively small, and it is quite possible that screening of a larger, more diverse library would identify other mutant proteins having properties similar to those of PA-GN and PA-NS.

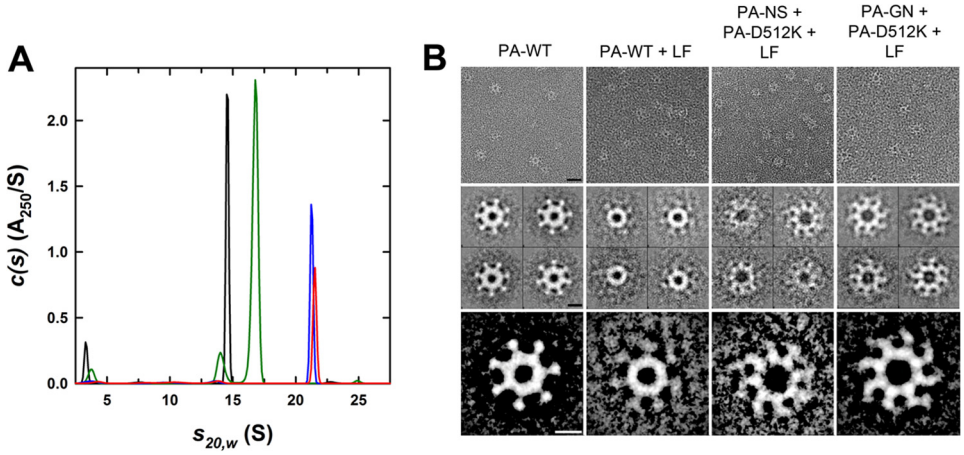

FIGURE 5. **Biophysical characterization of oligomeric PA variants.** *A*, characterization of PA and LF complexes by sedimentation velocity. Absorbance *c*(*s*) distributions obtained in SEDFIT for wild type PA oligomer at 1.32 mg/ml (*black*), wild type PA + LF 2.36 mg/ml (*green*), PA-D512K + PA-GN + LF at 0.74 mg/ml (*blue*), and PA-D512K + PA-NS +LF at 0.63 mg/ml (*red*). Each sample showed the presence of a predominant species. Similar profiles were observed using the interference optical system. *B*, EM images of heptameric and octameric PA species. The *top row* shows representative unprocessed cryo-EM images from the samples indicated. The *scale bar* is 20 nm and applies to this row only. The *middle row* shows the classes that resulted from the reference-free alignment, and the *bottom row* is a compressed overlay of the respective classes for each sample. *Scale bars* for *middle* and *bottom rows*, 5 nm.

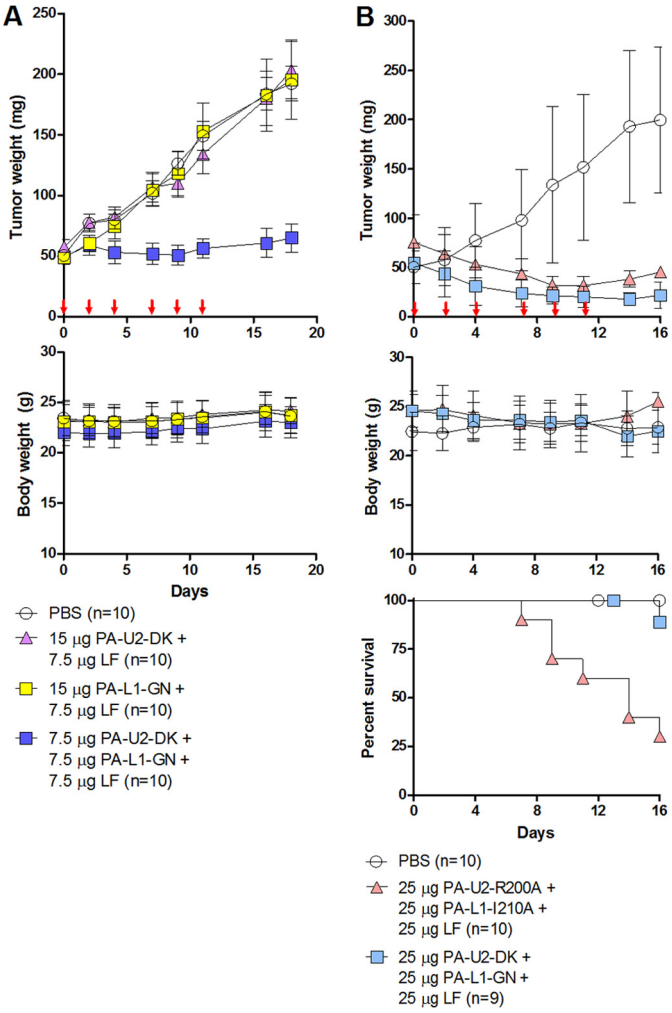

FIGURE 6. **Tumor targeting by complementary PA variants.** *A*, nude mice ($n = 10$/group) having 50-mg tumors composed of A549 cells (resulting from injection of 1×10^6 cells/animal intradermally) were injected IP on days 0, 2, 4, 7, 9, and 11 with PBS, 15 μg of PA and 7.5 μg of LF, or a combination of complementary PA variants (7.5 μg of each) and 7.5 μg of LF. Tumor weight and body weight were measured on these days. There were no animal deaths observed at this dose. *Error bars* denote S.D. *B*, nude mice ($n = 9$ or 10 per group) with tumors composed of A549 cells (from 5×10^6 cells/animal intradermally) were injected intraperitoneally using the same schedule as in *A* with PBS, the previously published intercomplementing system (25 μg of PA-U2-R200A + 25 μg of PA-L1-I210A + 25 μg of LF), or the octameric delivery system (25 μg of PA-U2-DK + 25 μg of PA-L1-GN + 25 μg of LF). Tumor weight, body weight, and survival were monitored. *Error bars* denote S.D.

Pore-forming toxins are often homo-oligomeric, with the prototypical example being staphylococcal α-hemolysin, a β-barrel pore-forming toxin (24). The staphylococcal α-hemolysin has been shown to form heptamers but under certain conditions will also form hexameric rings (25). Anthrax toxin was long thought to form heptamers exclusively (9), but the work by Krantz and colleagues (10, 11, 26, 27) has shown that functional octamers can also be formed, a conclusion that is confirmed and extended by these studies. This suggests a cautionary approach when considering the oligomeric states of other anthrax-like toxins, such as clostridial C2 toxin and iota toxin (28), and even all other pore-forming toxins, to include consideration that alternative oligomeric forms might be present in certain situations.

In principle, the mutagenesis and screening process described here can be repeated to create an octamer containing up to eight distinct specificity requirements for cell targeting. These steps could use some of the seven PA residues in addition to Asp-512, which were previously shown to prevent oligomerization when mutated to alanine (29, 30). One can envision using complementary PA variants similar to those described here as a platform to create "nano-toolboxes" for assembling several different proteins or enzymatic activities together in reproducible combinations to perform processes on the nanoscale. Also, these PA variants can be used to understand the specific receptor signaling requirements for uptake of anthrax toxin. Overall, this work provides the possibility of development and use of oligomers in targeting applications as presented here and enhances our understanding of toxin function and toxin-host interactions.

Acknowledgments—We thank David Garboczi and Apostolos Gittis for conducting dynamic light scattering experiments, D. Eric Anderson for determining intact masses of proteins, and Diane Guerrero and Inka Sastalla for thoughtful discussions.

REFERENCES

1. Fouet, A. (2009) The surface of *Bacillus anthracis*. *Mol. Aspects Med.* **30,** 374–385
2. Moayeri, M., and Leppla, S. H. (2009) Cellular and systemic effects of anthrax lethal toxin and edema toxin. *Mol. Aspects Med.* **30,** 439–455
3. Young, J. A., and Collier, R. J. (2007) Anthrax toxin: receptor-binding, internalization, pore formation, and translocation. *Annu. Rev. Biochem.* **76,** 243–265
4. Leppla, S. H. (1982) Anthrax toxin edema factor: a bacterial adenylate cyclase that increases cyclic AMP concentrations of eukaryotic cells. *Proc. Natl. Acad. Sci.* **79,** 3162–3166
5. Dumetz, F., Jouvion, G., Khun, H., Glomski, I. J., Corre, J. P., Rougeaux, C., Tang, W. J., Mock, M., Huerre, M., and Goossens, P. L. (2011) Noninvasive imaging technologies reveal edema toxin as a key virulence factor in anthrax. *Am. J. Pathol.* **178,** 2523–2535
6. Duesbery, N. S., Webb, C. P., Leppla, S. H., Gordon, V. M., Klimpel, K. R., Copeland, T. D., Ahn, N. G., Oskarsson, M. K., Fukasawa, K., Paull, K. D., and Vande Woude, G. F. (1998) Proteolytic inactivation of MAP-kinase-kinase by anthrax lethal factor. *Science* **280,** 734–737
7. Vitale, G., Bernardi, L., Napolitani, G., Mock, M., and Montecucco, C. (2000) Susceptibility of mitogen-activated protein kinase kinase family members to proteolysis by anthrax lethal factor. *Biochem. J.* **352,** 739–745
8. Levinsohn, J. L., Newman, Z. L., Hellmich, K. A., Fattah, R., Getz, M. A., Liu, S., Sastalla, I., Leppla, S. H., and Moayeri, M. (2012) Anthrax lethal factor cleavage of Nlrp1 is required for activation of the inflammasome. *PLoS Pathog.* **8,** e1002638
9. Milne, J. C., Furlong, D., Hanna, P. C., Wall, J. S., and Collier, R. J. (1994) Anthrax protective antigen forms oligomers during intoxication of mammalian cells. *J. Biol. Chem.* **269,** 20607–20612
10. Kintzer, A. F., Thoren, K. L., Sterling, H. J., Dong, K. C., Feld, G. K., Tang, I. I., Zhang, T. T., Williams, E. R., Berger, J. M., and Krantz, B. A. (2009) The protective antigen component of anthrax toxin forms functional octameric complexes. *J. Mol. Biol.* **392,** 614–629
11. Feld, G. K., Kintzer, A. F., Tang, I. I., Thoren, K. L., and Krantz, B. A. (2012) Domain flexibility modulates the heterogeneous assembly mechanism of anthrax toxin protective antigen. *J. Mol. Biol.* **415,** 159–174
12. Mogridge, J., Cunningham, K., Lacy, D. B., Mourez, M., and Collier, R. J. (2002) The lethal and edema factors of anthrax toxin bind only to oligomeric forms of the protective antigen. *Proc. Natl. Acad. Sci.* **99,** 7045–7048
13. Singh, Y., Chaudhary, V. K., and Leppla, S. H. (1989) A deleted variant of *Bacillus anthracis* protective antigen is non-toxic and blocks anthrax

toxin action *in vivo*. *J. Biol. Chem.* **264,** 19103–19107
14. Pomerantsev, A. P., Pomerantseva, O. M., Moayeri, M., Fattah, R., Tallant, C., and Leppla, S. H. (2011) A *Bacillus anthracis* strain deleted for six proteases serves as an effective host for production of recombinant proteins. *Protein Expr. Purif.* **80,** 80–90
15. Varughese, M., Chi, A., Teixeira, A. V., Nicholls, P. J., Keith, J. M., and Leppla, S. H. (1998) Internalization of a *Bacillus anthracis* protective antigen-c-Myc fusion protein mediated by cell surface anti-c-Myc antibodies. *Mol. Med.* **4,** 87–95
16. Park, S., and Leppla, S. H. (2000) Optimized production and purification of *Bacillus anthracis* lethal factor. *Protein Expr. Purif.* **18,** 293–302
17. Ho, S. N., Hunt, H. D., Horton, R. M., Pullen, J. K., and Pease, L. R. (1989) Site-directed mutagenesis by overlap extension using the polymerase chain reaction. *Gene* **77,** 51–59
18. Schuck, P. (2000) Size-distribution analysis of macromolecules by sedimentation velocity ultracentrifugation and Lamm equation modeling. *Biophys. J.* **78,** 1606–1619
19. Boukari, H., Nossal, R., Sackett, D. L., and Schuck, P. (2004) Hydrodynamics of nanoscopic tubulin rings in dilute solutions. *Phys. Rev. Lett.* **93,** 098106
20. Cole, J. L., Lary, J. W., P Moody, T., and Laue, T. M. (2008) Analytical ultracentrifugation: sedimentation velocity and sedimentation equilibrium. *Methods Cell Biol.* **84,** 143–179
21. Liu, S., Bugge, T. H., and Leppla, S. H. (2001) Targeting of tumor cells by cell surface urokinase plasminogen activator-dependent anthrax toxin. *J. Biol. Chem.* **276,** 17976–17984
22. Liu, S., Netzel-Arnett, S., Birkedal-Hansen, H., and Leppla, S. H. (2000) Tumor cell-selective cytotoxicity of matrix metalloproteinase-activated anthrax toxin. *Cancer Res.* **60,** 6061–6067
23. Liu, S., Redeye, V., Kuremsky, J. G., Kuhnen, M., Molinolo, A., Bugge, T. H., and Leppla, S. H. (2005) Intermolecular complementation achieves high-specificity tumor targeting by anthrax toxin. *Nat. Biotechnol.* **23,** 725–730
24. Song, L., Hobaugh, M. R., Shustak, C., Cheley, S., Bayley, H., and Gouaux, J. E. (1996) Structure of staphylococcal α-hemolysin, a heptameric transmembrane pore. *Science* **274,** 1859–1866
25. Czajkowsky, D. M., Sheng, S., and Shao, Z. (1998) Staphylococcal α-hemolysin can form hexamers in phospholipid bilayers. *J. Mol. Biol.* **276,** 325–330
26. Kintzer, A. F., Sterling, H. J., Tang, I. I., Williams, E. R., and Krantz, B. A. (2010) Anthrax toxin receptor drives protective antigen oligomerization and stabilizes the heptameric and octameric oligomer by a similar mechanism. *PLoS One* **5,** e13888
27. Feld, G. K., Thoren, K. L., Kintzer, A. F., Sterling, H. J., Tang, I. I., Greenberg, S. G., Williams, E. R., and Krantz, B. A. (2010) Structural basis for the unfolding of anthrax lethal factor by protective antigen oligomers. *Nat. Struct. Mol. Biol.* **17,** 1383–1390
28. Barth, H., Aktories, K., Popoff, M. R., and Stiles, B. G. (2004) Binary bacterial toxins: biochemistry, biology, and applications of common *Clostridium* and *Bacillus* proteins. *Microbiol. Mol. Biol. Rev.* **68,** 373–402
29. Mogridge, J., Mourez, M., and Collier, R. J. (2001) Involvement of domain 3 in oligomerization by the protective antigen moiety of anthrax toxin. *J. Bacteriol.* **183,** 2111–2116
30. Ahuja, N., Kumar, P., and Bhatnagar, R. (2001) Hydrophobic residues Phe552, Phe554, Ile562, Leu566, and Ile574 are required for oligomerization of anthrax protective antigen. *Biochem. Biophys. Res. Commun.* **287,** 542–549
31. Lacy, D. B., Wigelsworth, D. J., Melnyk, R. A., Harrison, S. C., and Collier, R. J. (2004) Structure of heptameric protective antigen bound to an anthrax toxin receptor: a role for receptor in pH-dependent pore formation. *Proc. Natl. Acad. Sci.* **101,** 13147–13151
32. Singh, Y., Klimpel, K. R., Goel, S., Swain, P. K., and Leppla, S. H. (1999) Oligomerization of anthrax toxin protective antigen and binding of lethal factor during endocytic uptake into mammalian cells. *Infect. Immun.* **67,** 1853–1859